J. Plasma Physics (2012), vol. 78, part 4, pp. 441–445. © Cambridge University Press 2012
doi:10.1017/S0022377812000414

Sensitivity study in a compact accelerator for laser-generated protons

P. ANTICI[1,2], M. MIGLIORATI[1,2], A. MOSTACCI[1,2], L. PICARDI[3], L. PALUMBO[1,2] and C. RONSIVALLE[3]

[1]Istituto Nazionale di Fisica Nucleare (INFN), Via E. Fermi, 40 - 00044 Frascati, Rome, Italy (patrizio.antici@uniroma1.it)
[2]Dipartimento di Scienze di Base e Applicate per l'Ingegneria (SBAI), 'Sapienza' Università di Roma, Via Scarpa 14-16, 00161 Rome, Italy
[3]ENEA Frascati, Via Enrico Fermi 45 - 00044 Frascati, Rome, Italy

(Received 30 September 2011; revised 24 February 2012; accepted 5 March 2012; first published online 1 May 2012)

Abstract. A sensitivity study is presented here on a compact hybrid postacceleration scheme coupling laser-generated protons to a high frequency Linac based on the use of a SCDTL (Side Coupled Drift Tube Linac) structure. The study analyzes the main laser-generated beam characteristics and the most important parameters linked to the accelerating structure. We show that the required tolerances regarding alignment and field uniformity, although challenging, are within the reach of actual technology. Regarding the laser-generated proton beam parameters (spot size and divergence), we show that they have only a little influence on the final emittance that is mainly determined by the capturing and accelerating structure. However, these parameters can sensitively affect the final transmission of the proton beam current.

The generation of laser-driven proton beamlines is a subject of increasing interest within the accelerator community since they benefit from the compactness, efficiency, and versatility of a laser-based proton source, therefore, reducing costs, size, and complexity compared to conventional accelerator structures. Laser-generated protons are produced by irradiation of thin solid foils with an ultraintense ($>10^{18}$ W cm^{-2}) ultrashort laser pulse (30 fs to 10 ps). Energies in excess of 60 MeV with very low emittance (<0.2 mm mrad rms) have been measured on different high-energy laser facilities [1]. The drawback of these laser-generated proton sources is a very large energy spread (from 100% up to 5–7%) and its large divergence (up to $\sim$ 20%). Therefore, at present, these beams cannot be directly used as proton source and cannot be considered as complete replacement for the conventional proton accelerator facilities.

Over the past few years, several attempts have been made to improve the characteristics of the laser-generated proton beams [2] in order to obtain better control of the beam properties and, thus, make them comparable to those of conventional accelerators. Besides working on the proton source itself, i.e. on the interaction target or interaction laser, much effort is now being put on improving their properties with conventional accelerator devices, such as quadrupoles, solenoids, and linear accelerator devices (e.g. Drift Tube Linacs, DTL). Preliminary theoretical studies have already been carried out, showing that laser-generated protons can indeed be captured and postaccelerated in conventional accelerator devices [3], generating a 'hybrid accelerator'. A more recent work has analyzed the possibility of using more compact hybrid accelerating structures, particularly designed for medical purposes [4].

Although laser facilities are making laser-driven beamlines a main priority of their scientific case, to our knowledge, not all studies normally performed on conventional beamlines have been carried out, including sensitivity studies. In our paper, we have taken the beamline used in [4] to perform this study, since we consider it to be an important step for evaluating the reliability of the accelerator and in case identify key elements/parameters on which close attention needs to be put. We could repeat the current study with different laser-produced parameters. From previous studies performed for the TOP project [5], we know that for higher injected proton energies (e.g. 18–20 MeV), the tolerances (including for the PMQs) would be more relaxed.

In this paper, we have performed sensitivity studies to evaluate how a variation of the nominal parameters on the plasma source or the accelerating structure affects the final properties of the outcoming beam. We have concentrated only on the sensibility downstream the targetry. The sensibility and reliability of the source and the laser–matter interaction (i.e. the laser pointing and in case the targetry) are not considered and are evaluated separately. Indeed, the laser pointing depends heavily on the laser properties while the targetry is intrinsically dependent on the type of experiment. We have, therefore, uncoupled the sensitivity of the accelerating structure from the sensitivity of the targetry.

For the study, we have used a compact hybrid proton accelerator described in [4]. This accelerator is based on a laser-driven plasma source that is coupled to

https://doi.org/10.1017/S0022377812000414 Published online by Cambridge University Press

Table 1. Parameters of the laser-generated proton beam.

Parameter	Value
Energy	7.0 ± 0.1 MeV
rms unnormalized emittance	0.18 mm-mrad
rms Spot size $\sigma_x = \sigma_y$	20 μm
rms divergence $\sigma_{x'} = \sigma_{y'}$	9 mrad
Number of protons	210^9
Charge	320 pC

Table 2. SCDTL structure parameters.

Parameter	Value
Number of modules	2
Number of tanks/module	11
Number of cells/tank	4
Intertank distance	4.5 $\beta\lambda$ in module #1, 4.5–3.5 $\beta\lambda$ in module #2
Bore radius	2 mm in module #1, 2.5 mm in the module #2
Total length	2.59 m
Average electric field, E_0	11.3 MV m^{-1}
Acc. electric field, E_0T	between 7 and 7.75 MV m^{-1}
Synchronous phase, φ_s	$-30°$
Maximum PMQ gradient	220 T m^{-1}
RF power for the structure	<1.5 MW

a conventional accelerator structure particularly suited for medical purposes (Side Coupled Drift Tube Linacs, SCDTL, see later). A schematic of the full accelerator is shown in Fig. 1. For the proton source, we have used a laser-generated proton source using typical protons generated by a 100 TW, standard contrast laser, with proton parameters as reported in [3]. The laser-generated protons are shaped at the source using a 'microlens', i.e. a device that collimates and monoenergized the laser-driven proton beam [6, 11]. The microlens being very close to the proton generating target (<1 cm), we have considered this element to be part of the targetry. The targetry of those experiments being very complex [7, 8] and depending from experiment to experiment, we have not investigated its sensibility, for a detailed description of the individual parameters we refer to the dedicated literature.

We have adopted this proton source configuration, since the achieved proton parameters were, all combined, the best currently obtained compromise in terms of monochromaticy, emittance, and energy and were fully described. The experimentally measured characteristics of protons source are reported in Table 1 [3]; a spectrum, before and after the microlens, can be found in [4]. After the proton source, we have considered a drift space of 17 mm. This drift space is needed for technical issues and has shown to be an optimized distance to the next element. After the drift space, we have placed a solenoid as used in [9]. The solenoid has the function of collecting the protons prior to injecting them in the transport and accelerating structure. Consistent with the postaccelerating structure in [4], we have used a short focusing system based on a solenoid (with the same characteristics of the PHELIX solenoid, i.e. a length of 7 cm with an aperture diameter of 4.4 cm) with its corner at a distance of 17 mm away from the targetry. The capturing solenoid is followed by a 2998 MHz SCDTL structure, with characteristics indicated in Table 2, placed at 11.7 cm from the solenoid exit, accelerating the beam up to 15.5 MeV for a total beamline length of ~3 m. We are aware that our hybrid proton beamline could have been designed with a different laser-generated proton source, provided all relevant parameters were available. But the numerical particle tracing codes being very sensitive to the input parameters, the design of a lattice structure based on only estimative parameters would have no sense. Moreover, it was our aim to analyze the sensitivity of an already studied hybrid accelerator.

Several tolerance parameters have been taken into account for the sensitivity study. We considered first the tolerance parameters of the proton beam parameters at the entrance of the accelerating section, i.e. variations of the beam waist (σ_x) and of the beam divergence ($\sigma_{x'}$), where cylindrical symmetry is assumed. Then we consider tolerances due to the lattice structure, in particular

(1) The stability of the permanent quadrupole magnet (PMQ) field, i.e. deviations of its gradient from the nominal one;

(2) The transverse displacement (x, y) of the PMQ from its nominal axis;

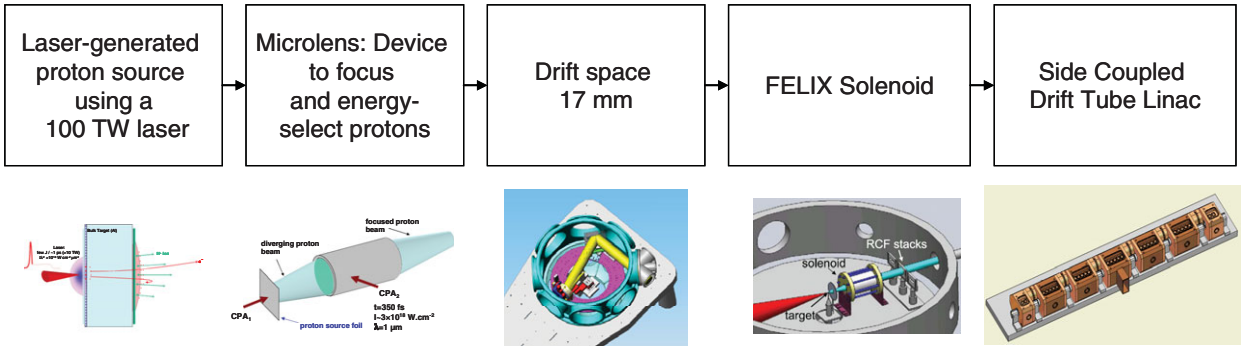


Figure 1. (Colour online) Schematic of the accelerator, showing the laser-driven proton source, the microlens, the Solenoid for the proton capture and the SCDTL for the transport and postacceleration.

https://doi.org/10.1017/S0022377812000414 Published online by Cambridge University Press

(3) The fluctuation of the electric field located inside the accelerating tank.

We have considered deviations from the ideal, optimized case. In that case, PMQ are considered not to move from its optimized position and keep nominal parameters without fluctuation. Fluctuations are considered to be globally found inside the structure, i.e. for the transverse displacement (x, y) of the PMQ from its nominal axis, any PMQ is considered, not only the first one.

As output criteria for judging the quality of the beam, we have considered its emittance and the transmitted current. We have taken as nominal parameters the transverse input parameters indicated in [4].

In order to evaluate the sensitivity of the laser-generated proton beam parameters for the entire lattice structure, we have performed a series of simulations using the tracking code TSTEP [10] and considering a total number of Np = 300 000 macroparticles. The sensitivity study on the source has been achieved varying the input rms unnormalized emittance $\varepsilon_{\mathrm{un}} = \sigma_x \sigma_{x'}$, i.e. varying $\sigma_x, \sigma_{x'}$ or both and has been performed for an input current of 200 mA which would represent the ideal maximum current achievable with the current proton source [4]. In this reference, it has already been shown that for this input current the used transport line has low efficiency. Table 3 reports the results of the study: the first row corresponds to the results obtained with the reference parameters (such as indicated in Table 1, $\sigma_x = 20$ μm and $\sigma_{x'} = 9$ mrad), while the other rows refer to cases where either the emittance or the beam spot size have been artificially increased by a factor of 2. An increase of the proton spot size is possible when changing the laser parameters at the source. Since protons stem out normally to the target, a larger laser spot size would generate a larger proton beam. In the present case, the proton source had been generated using a microlens. Modifying the properties of the microlens allowed achieving different proton spot sizes and different divergences [11].

One can see from Table 3 that despite the higher initial emittance, a larger spot size improves the total and useful transmission with respect to the nominal case. As in [4], the useful current is defined as the amount of the transmitted current within a window of 0.6 MeV centered around the energy where the particle density is at its maximum. This is due to lower space charge effects that become less dominant for larger beam sizes. On the other side, in the case of a larger beam spot and also a larger beam divergence (case 4), beam losses are more pronounced. However, since for the very small nominal beam size (20 μm) the space charge effect is dominating, the influence of the spot size is predominant to the effect of the beam divergence. As a result, Table 3 shows that the final normalized emittance for all considered cases is not very sensitive to the input conditions.

One can compare the TSTEP outputs (transverse particle distribution and phase space) for the reference case ($\sigma_x = 20$ μm and $\sigma_{x'} = 9$ mrad) with those obtained using the run performed with $\sigma_x = 40$ μm and $\sigma_{x'} = 9$ mrad (see Fig. 2) which indeed shows the best results in terms of transmission. The figure shows four plots: initial spot size, longitudinal phase space and spot size at the SCDTL entrance, spot size at the SCDTL output for the two beam conditions. The effects of having a larger input spot size are evident in terms of reduction of longitudinal emittance dilution (i.e. reduction of length and energy spread of the beam) and spot size at the linac entrance resulting in a more efficient transport within the postaccelerating section and a negligible broadening of the spot size at the exit of the accelerator.

We now study the sensitivity of the system to different types of tolerances within the accelerating section (SCDTL). We have adopted the same approach as used when studying similar accelerating devices inserted in a proton therapy linac injected by a conventional low-current injector [12].

The analysis consists in a statistical scan on the following three parameters that can mainly affect the beam transmission: quadrupole gradients values, quadrupole transverse position, electric field amplitude in the tanks. For each parameter considered in the analysis, 50 runs have been performed assigning random values uniformly distributed in the range $\pm$ |Error amplitude| for different maximum values of the error amplitude (total quantity of runs = 50 times the number of error amplitudes). The study has been done again for an input current of 200 mA. In the numerical calculations, the number of macroparticles has been reduced to 30 000 in order to lower the computational time for calculations. However, this number is sufficient to allow a detailed statistic and to retrieve the parameter under analysis, i.e. the relative transmission (RT). The RT is defined as the transmission normalized to the maximum capture, i.e. when all sensitivity parameters are nominal (best case).

The results of this study are summarized in the plots of Figs. 3 and 4. The plots show the minimum (worst case)

Table 3. Computed output transmission for different initial beam parameters.

Case	Input σ_x (μm)	Input $\sigma_{x'}$ (mrad)	Input rms unnormalized emittance (mm-mrad)	Total output current (mA)	Useful output current (mA)	Output rms normalized emittance $(E_{xn} \times E_{yn})^{0.5}$ (mm-mrad)
1	20	9	0.18	37	13	0.264
2	40	9	0.36	64	26	0.197
3	20	18	0.36	30	10	0.210
4	40	18	0.72	47	20	0.209

https://doi.org/10.1017/S0022377812000414 Published online by Cambridge University Press

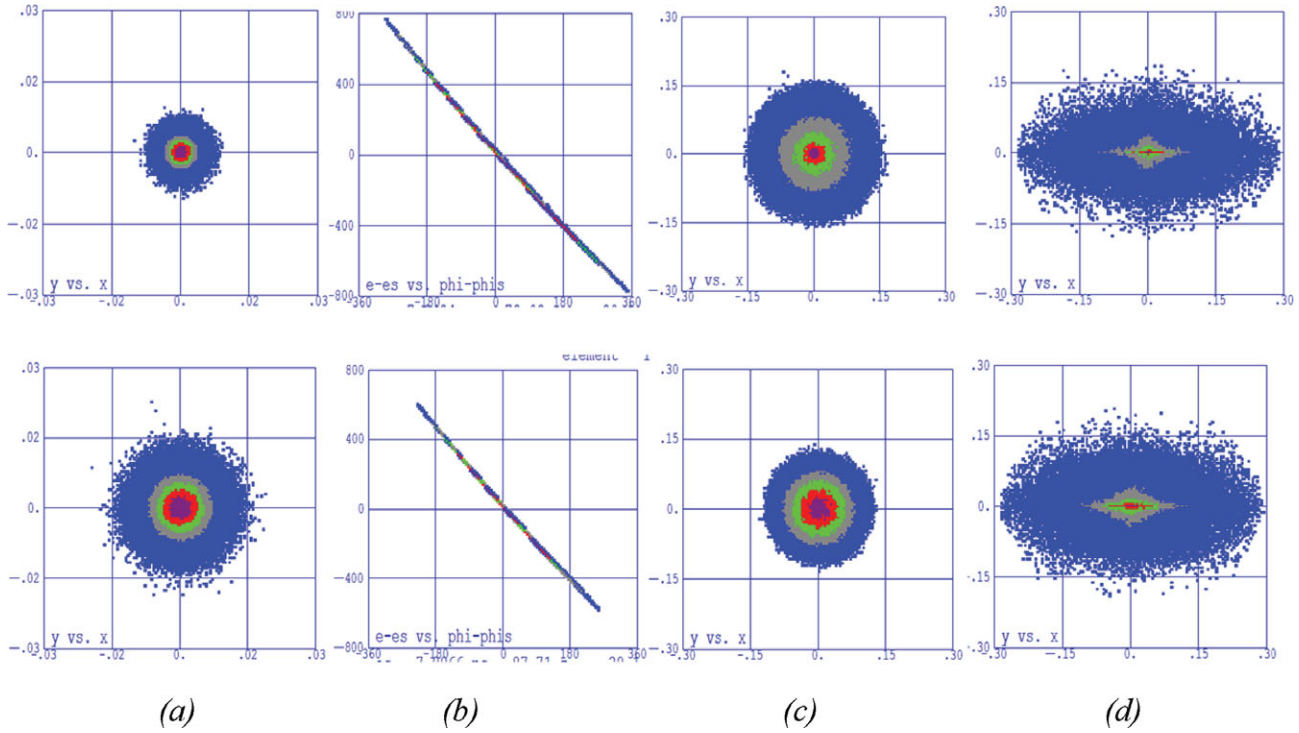


Figure 2. (Colour online) TOP plots: input beam parameters $\sigma x = 20$ μm, $\sigma x' = 9$ mrad, BOTTOM plots: input beam parameters $\sigma_x = 40$ μm, $\sigma_{x'} = 9$ mrad; (a) transverse beam size y vs. x at the laser-driven proton source (b) ΔE vs. $\Delta\varphi$ at the SCDTL entrance, i.e. after the matching section (c) y vs. x at the SCDTL entrance, i.e. after the matching section (c) y vs. x at SCDTL exit. The units are keV for energy, RF deg for phase, cm for coordinates. The limits of the scale for the y vs. x plots are 0.03 cm for the input coordinates and 0.3 cm for the coordinates at the linac entrance and exit.

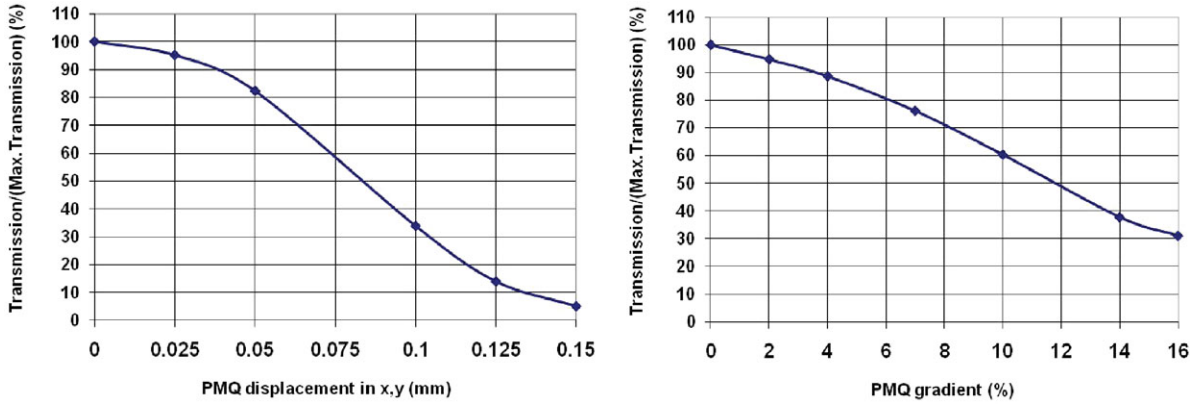


Figure 3. (Colour online) Effect of PMQ errors: minimum relative transmission on 50 runs vs. parameter error for (a, left) transverse displacement (b, right) gradient.

RT (averaged over 50 runs) versus tolerance parameters: Fig. 3(a) considers the tolerance regarding the PMQs transverse displacement while Fig. 3(b) considers the effect of different PMQ gradients. Fig. 4 analyzes the tolerance with respect to deviations in the electric field amplitude. For each sensitivity parameters, we define as the maximum accepted tolerance when the RT becomes below 95%.

The maximum accepted tolerances on the investigated parameters retrieved using the above mentioned criteria and extracted from Figs. 3 and 4 are reported in Table 4. In comparison with other tolerance parameters common for conventional accelerators, it appears that the most critical parameter is the PMQs displacement. This, however, imposes alignment constraints within available technology, since tolerances have to be respected within short distances (tank-to-tank) but not necessarily within long distances. The manufacturer standards guarantee tolerances within 50 μm, which worsens the transmission by $\sim$15% more than a tolerance of 25 μm, producing still acceptable results. Moreover, manufacturers are now aiming at tolerances reaching 25 μm. The general dimensions involved are very small: a bore hole of 2 mm in the first module and 2.5 mm in the second module. They are imposed by the need to confine the electric field in the region of the cell by reducing the 'fringing'

https://doi.org/10.1017/S0022377812000414 Published online by Cambridge University Press

Table 4. Single parameters tolerances.

Parameter	Tolerance
PMQ gradient	±2%
PMQ x-y displacement	±25 μm
Tank field amplitude error	±4%

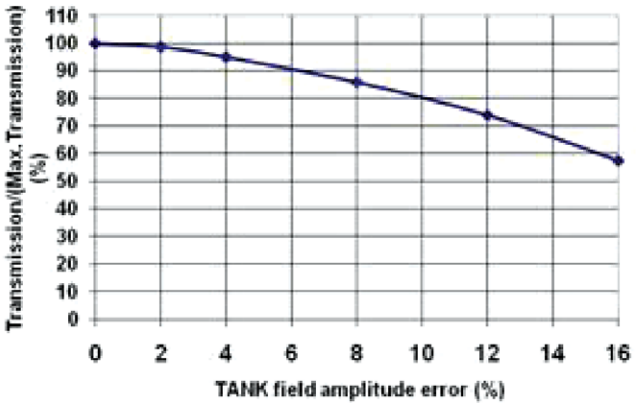


Figure 4. (Colour online) Effect of tank electric field amplitude error: minimum relative transmission on 50 runs vs. parameter error.

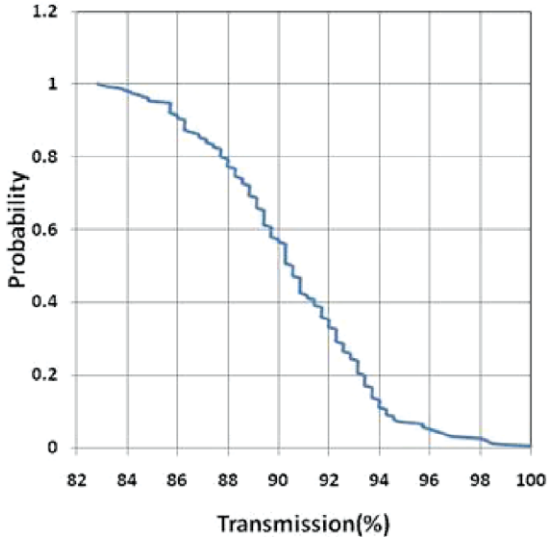


Figure 5. (Colour online) Effect of errors equal to tolerances in terms of probability to get a relative transmission larger than the abscissa value.

and, thus, avoiding to reduce the transit time, since the 'fringing' increases with decreasing ratio of the cell length/bore hole radius.

We have further performed an analysis over 150 runs in which all three above mentioned parameters have been randomly varied within the tolerance ranges. As output, we have again considered the RT of the proton beam and statistically assessed the probability of achieving at least the predetermined transmission. Fig. 5 shows the probability versus minimum RT. We see that with the current configuration, we have ∼50% of probability of achieving a minimum transmission of 90%, i.e. $13 \times 0.9 = 11.7$ mA. If, however, we lower the expected transmission to 85%, i.e. 11 mA, we see that this event is likely to happen in ∼95% of the cases.

References

[1] S. A. Gaillard et al. 2011 *Phys. Plasmas* **18**, 056710.

[2] Schwoerer, H., Pfotenhauer, S., Jäckel, O., Amthor, K.-U., Liesfeld, B., Ziegler, W., Sauerbrey, R., Ledingham, K. W. D. and Esirkepov, T. 2006 *Nature* (London) **439**, 445; Patel, P. K., Mackinnon, A. J., Key, M. H., Cowan, T. E., Foord, M. E., Allen, M., Price, D. F., Ruhl, H., Springer, P. T. and Stephens, R. 2003 *Phys. Rev. Lett.* **91**, 125004; Schollmeier, M., Becker, S., Geißel, M., Flippo, K. A., Blažević, A., Gaillard, S. A., Gautier, D. C., Grüner, F., Harres, K. Kimmel, M. et al. 2008 *Phys. Rev. Lett.* **101**, 055004; Ter-Avetisyan, S., Schnürer M., Polster, R., Nickles, P. V. and Sandner, W. 2008 *Laser Part. Beams* **26**, 637; Harres, K., Alber, I., Tauschwitz, A., Bagnoud, V., Daido, H., Günther, M., Nürnberg, F., Otten, A., Schollmeier, M. Schütrumpf, J. et al. 2010 *Phys. Plasmas* **17**, 23107; Nakamura, S., Ikegami, M., Iwashita, Y., Shirai, T., Tongu, H., Souda, H., Daido, H., Mori, M., Kado, M. Sagisaka, A. et al. 2007 *Jap. J. Appl. Phys.* **46**, L717; Nishiuchi, M., Sakaki, H., Hori, T., Bolton, P. R., Ogura, K., Sagisaka, A., Yogo, A., Mori, M., Orimo, S. Pirozhkov, A. S. et al. 2010 *Phys. Rev. ST AB* **13**, 071304.

[3] Antici, P., Fazi, M., Lombardi, A., Migliorati, M., Palumbo, L., Audebert, P. and Fuchs, J. 2008 *J. Appl. Phys.* **104**, 124901.

[4] Antici, P., Migliorati, M., Mostacci, A., Picardi, L., Palumbo, L. and Ronsivalle, C. 2011 *Phys. Plasmas* **18**, 073103.

[5] Picardi, L., Orlandi, G., Ronsivalle, C. and Vignati, A. 1996 *Proc. of the European Particle Accelerator Conference 1996*. Barcelona: JACoW, THP049G.

[6] Willi, O., Toncian, T., Borghesi, M., Fuchs, J., D'humières, E., Antici, P., Audebert, P., Brambrink, E., Cecchetti, C. Pipahl, A. et al. 2007 *Laser Part. Beams* **25**, 71–77.

[7] Cecchetti, C. A., Borghesi, M., Fuchs, J., Wilson, P. A., Antici, P., Audebert, P., Romagnani, L., Willi, O., Toncian, T. Young, R. et al. 2009 *Phys. Plasmas* **16**, 043102.

[8] Antici, P., Fuchs, J., Borghesi, M., Gremillet, L., Grismayer, T., Sentoku, Y., d'Humières, E., Cecchetti, C. A., Mancic, A.Pipahl, A. C. et al. 2008 *Phys. Rev. Lett.* **101**, 105004.

[9] Bagnoud, V., Aurand, B., Blazevic, A., Borneis, S., Bruske, C., Ecker, B., Eisenbarth, U., Fils, J., Frank, A. Gaul, E. et al. 2009 *Appl. Phys.* B, doi: 10.1007/s00340-009-3855-7.

[10] Young, L. M., Los Alamos National Laboratory report LA-UR-96-1835.

[11] Toncian, T., Borghesi, M., Fuchs, J., d'Humieres, E., Antici, P., Audebert, P., Brambrink, E., Cecchetti, C. A., Pipahl, A. Romagnani, L. et al. 2006 *Science* **312**, 410.

[12] Ronsivalle, C., Carpanese, M., Marino, C., Messina, G., Picardi, L., Sandri, S., Basile, E., Caccia, B., Castelluccio, D. M., Cisbani, E., Frullani, S., Ghio, F., Macellari, V., Benassi, M., D'Andrea, M. and Strigari, L. 2011 The TOP-IMPLART Project. *Eur. Phys. J. Plus* **126** (7), 68.

https://doi.org/10.1017/S0022377812000414 Published online by Cambridge University Press